TU Delft

Delft University of Technology

Validation of the SU2 Fluid Dynamic Solver for Isentropic Non-Ideal Compressible Flows

Fuentes-Monjas, Blanca; Head, Adam J.; Servi, Carlo De; Pini, Matteo

DOI
10.1007/978-3-031-30936-6_10

Publication date
2023

Document Version
Final published version

Published in
ERCOFTAC Series

Citation (APA)
Fuentes-Monjas, B., Head, A. J., Servi, C. D., & Pini, M. (2023). Validation of the SU2 Fluid Dynamic Solver for Isentropic Non-Ideal Compressible Flows. In M. White (Ed.), *ERCOFTAC Series* (pp. 91-99). (ERCOFTAC Series; Vol. 29). Springer. https://doi.org/10.1007/978-3-031-30936-6_10

Important note
To cite this publication, please use the final published version (if applicable).
Please check the document version above.

Copyright
Other than for strictly personal use, it is not permitted to download, forward or distribute the text or part of it, without the consent of the author(s) and/or copyright holder(s), unless the work is under an open content license such as Creative Commons.

Takedown policy
Please contact us and provide details if you believe this document breaches copyrights.
We will remove access to the work immediately and investigate your claim.

This work is downloaded from Delft University of Technology.
For technical reasons the number of authors shown on this cover page is limited to a maximum of 10.

Green Open Access added to TU Delft Institutional Repository

'You share, we take care!' - Taverne project

https://www.openaccess.nl/en/you-share-we-take-care

Otherwise as indicated in the copyright section: the publisher is the copyright holder of this work and the author uses the Dutch legislation to make this work public.

Validation of the SU2 Fluid Dynamic Solver for Isentropic Non-Ideal Compressible Flows

Blanca Fuentes-Monjas[1], Adam J. Head[1(✉)], Carlo De Servi[1,2], and Matteo Pini[1]

[1] Propulsion and Power, Delft University of Technology, Delft, The Netherlands
{a.j.head,c.m.deServi,m.pini}@tudelft.nl
[2] Energy Technology Unit, VITO, Mol, Belgium
carlo.deservi@vito.be

Abstract. This work assessed the accuracy of the SU2 flow solver in predicting the isentropic expansion of Siloxane MM through the converging-diverging nozzle test section of the Organic Rankine Cycle Hybrid Integrated Device (ORCHID) [9]. The expansion is modeled using compressible Euler equations, and assuming adiabatic flow, while the fluid thermodynamic properties are estimated using the Peng-Robinson equation of state. The boundary conditions for the experiment and simulations correspond to a stagnation temperature and pressure of $\bar{T}_0 = 253.7\ ^\circ\mathrm{C}$ and $\bar{P}_0 = 18.36$ bar. At these inlet conditions the compressibility factor of the fluid is $Z_0 = 0.58$. The back pressure was equal to $\bar{P}_\mathrm{b} = 2.21$ bar. The Mach number along the centreline, and static pressure along the nozzle surface were used as the system response quantities for the validation exercise. The studied SU2 model provides valid predictions for Mach number and static pressure. The largest deviation observed in the Mach number comparison between the simulation and experiment is in the uniform flow region of the nozzle and is equal to $E_\mathrm{Mach} = 0.045$. Regarding the pressure trend, the largest discrepancy occurs in the kernel region and is equal to $E_\mathrm{pressure} = 9$ kPa. At the same time, the simulated Mach number and static pressure reach a maximum absolute uncertainty of ± 0.015 and of ± 20 kPa, respectively. For both quantities, these values are reached in the region close to the throat. All the uncertainties calculated for the simulated pressure profile were larger than those of the experiments. The static pressure is particularly sensitive to the geometrical uncertainties of the nozzle profile, especially inside the kernel region. A proper characterisation of the nozzle geometry was therefore required to perform a meaningful validation of the fluid dynamic solver. The developed infrastructure can be used in the future for the validation of SU2 in different operating conditions and flow cases.

Keywords: Validation · CFD · error identification and uncertainty estimation

1 Introduction

The organic Rankine cycle (ORC) turbogenerator based on high-speed turbomachinery is a promising technology for waste heat recovery. The design optimization of the turbine is key to achieve high conversion efficiency. However, the design of these machines is complicated by the occurrence of highly non ideal supersonic flows. At the same time,

© The Author(s), under exclusive license to Springer Nature Switzerland AG 2023
M. White et al. (Eds.): NICFD 2022, ERCOFTAC 29, pp. 91–99, 2023.
https://doi.org/10.1007/978-3-031-30936-6_10

the predictive capability of fluid dynamic solvers has not yet been rigorously assessed for these kinds of flows. As an effort in this direction, the present study focuses on the validation of the open-source CFD software SU2. Differently from the validation methodology adopted by [8], a novel mixed-uncertainty approach is employed to study the propagation of critical point properties, boundary conditions and geometric uncertainties through the computational model. The uncertainties related to the critical point properties of the fluid are considered *epistemic* uncertainties, while those associated with the boundary conditions of the experiment, as well as geometric uncertainties of the nozzle profile, constitute the *aleatory* uncertainties. These were propagated through the model using stochastic collocation. In particular, the uncertainties related to the manufacturing tolerances are modeled as in [6]. Regarding the experimental data, those pertaining to an experiment carried out in the ORCHID facility [9] and consisting of a supersonic expansion of the organic fluid hexamethyldisiloxane (MM) were considered. The validation exercise accounts also for the numerical uncertainties due to the discretization error, which were calculated using Richardson extrapolation.

The paper is structured as follows. Section 2 reports the SU2 NICFD model and the proposed uncertainty quantification and validation framework. The focus is set on the characterization and treatment of the relevant uncertainties within the validation experiment to achieve a meaningful comparison between experimental and numerical data. The results of the proposed validation workflow are presented in Sect. 4, where pressures and Mach number from the simulations are compared against the recorded experimental data. Finally, Sect. 5 reports relevant conclusions, and possible improvements that would allow for a more robust validation of the solver.

2 Model Definition and Validation Methodology

2.1 Validation Experiment

The test case considered in this work for the validation of SU2 is the expansion process of a dense vapour (siloxane MM) occurring in a planar converging-diverging nozzle. The measured quantities are the static pressure along the nozzle profile, and the Mach number along the nozzle mid-plane. The operating conditions targeted in the experiments are those corresponding to the design point of the nozzle. Notably, the total conditions at the inlet are $T_0 = 252\ ^\circ\mathrm{C}$, $P_0 = 18.4\ \mathrm{bar}$, while the back pressure is $2.1\ \mathrm{bar}$. The nozzle throat is 20 mm by 7.5 mm (W x H), see [10] for more details about the nozzle geometry and experiment.

2.2 CFD Model

The flow in the nozzle is modeled as inviscid and two-dimensional to reduce the computational cost of the uncertainty quantification study. This assumption is justified also by the work of [9] and [3], where the results obtained for viscous versus inviscid, 2D versus 3D flow models of the nozzle are compared. The simulations performed in this work were carried out with the open-source SU2 solver Economon *et al*. [7] previously extended and verified for simulating NICFD flows by Pini *et al*. [14].

The calculation of the thermodynamic properties of the fluid requires the selection of a suitable *equation of state*. In this case, the polytropic (constant c_p) cubic Peng-Robinson equation of state available in SU2 was selected. The variation of c_p along the expansion process was found to be limited for the considered thermodynamic conditions. Thus, the use of a non-polytropic model was discarded to reduce the computational cost of the simulations. More specifically, the specific heat ratio was set to $\gamma = 1.0265$. Inlet/outlet Riemann boundary conditions were imposed in the simulations. For the convective fluxes the upwind Roe scheme generalized for non-ideal gases is employed together with a MUSCL reconstruction to achieve second order accuracy. The spatial gradients required by the MUSCL scheme are computed using weighted least squares. The Venkatakrishnan limiter is set to 0.3. More details regarding the solver configuration for NICFD can be found in [16].

A grid convergence study based on the methods given in [1,4] was performed to determine the optimum unstructured mesh distribution. The results of this study, which are reported in [3], showed that about forty thousands elements were required to keep a reasonable balance between numerical uncertainty and computational cost. The CFD simulations were performed on a server class AMD Opteron 6234 (2.4 Ghz, 48 cores) with 192 GB of memory.

3 Model Uncertainties

The model input uncertainties included in this study pertain to: the total inlet conditions (T_0, P_0), the critical properties used in the thermodynamic model (P_{cr}, T_{cr}) to determine the parameters of the *cubic equation of state*, and the nozzle geometry. The uncertainty associated with the critical point properties is treated as epistemic, while the other uncertainty sources are assumed aleatory.

The average and standard deviation of the normal distribution associated to the total inlet conditions are computed from the values measured inside the settling chamber of the ORCHID nozzle test section [10]. The average and the probability distribution functions of the total conditions (T_0, P_0) derived from the experiment are $\mathcal{N}(526.85, 0.3295)$ K, $\mathcal{N}(18.36, 0.01145)$ bar. The only value set as deterministic is the nozzle back pressure, fixed at a value of $\overline{P}_{\text{b}} = 2.21$ bar.

The intervals assigned to the critical point temperature and pressure are chosen based on the minimum and maximum experimental data reported in the literature. The corresponding intervals are $T_{\text{cr}} = [518.5,\ 521.6]$ K and $P_{\text{cr}} = [18.9,\ 19.27]$ bar. The lower bounds were determined by taking the minimum value of critical pressure [5] and temperature [12] and subtracting to these values the expanded uncertainty (two times the standard deviation) calculated considering the experimental data in the literature. An equivalent procedure was used to calculate the upper bound. No probability distribution is assigned to *epistemic* uncertainties.

The possible errors during the manufacturing of the nozzle profile are included in the UQ study using a modified version of the model proposed in [6]. The adapted model describes the deviation in the normal direction of the manufactured nozzle profile with respect to the nominal one, Δ, by means of a Gauss Random field. A Gauss Random field is completely defined by its average and covariance function, which is approximated by a Karhunen-Loève expansion, as

$$\Delta(s,\omega) = \bar{\Delta}(s,\omega) + C(s,x) = \bar{\Delta}(s,\omega) + \sum_{i=1}^{\infty} \sqrt{\lambda_i}\Phi_i(s)Z_i(\omega), \tag{1}$$

where s is the profile surface parametrization coordinate, being $s = 0$ at the nozzle inlet and $s = 1$ at the outlet. The terms λ_i and $\Phi_i(s)$ are the eigenvalues and eigenfunctions of the covariance function $C(s,x)$ respectively, while $Z_i(\omega)$ are the coefficients of the expansion which are defined by standard normal distributions, $\mathcal{N}(0,1)$. The calculation of λ_i and $\Phi_i(s)$ is done by solving the Fredholm integral of the second kind using the Nÿstrom method [13].

$$\int_0^1 C(s,x)\Phi_i(x)dx = \lambda_i\Phi_i(s) \tag{2}$$

The integral in the previous equation is calculated using the algorithm described in [2] and considering a Gaussian quadrature with 500 points. The covariance in this model is defined as

$$C(s_1,s_2) = \sigma^2 \cdot \rho(s_1,s_2), \tag{3}$$

where σ is the tolerance of the manufacturing process and $\rho(s_1,s_2)$ is the correlation function that is modeled with the following squared exponential

$$\rho(s_1,s_2) = \exp\left(\frac{-|s_1-s_2|^2}{L(s_1)\cdot L(s_2)}\right) \tag{4}$$

$$L(s) = L_0 + (L_T - L_0)\cdot \exp\left(\frac{-|s-s_{\text{throat}}|^2}{\omega^2}\right). \tag{5}$$

The parameters L_0, L_T and ω are normalized using the total nozzle surface length. Their values, that were set equal to 0.25, 0.025 and 0.25, respectively, in this study, are generally the result of a fitting procedure based on repeated measurements of the shape of the component of interest. This was, however, beyond the scope of the present work. The nozzle profiles were measured only once with a ball point probe [17]. The constants in 5 were then calibrated based on the limited data available and qualitative considerations based on the work in [6]. The tolerance, σ, was, instead, set to be 1.5×10^{-5} m based on the accuracy of the ball point probe used to measure the nozzle profiles.

The number of terms used for the truncated Karhunen-Loève expansion, Eq. 1, is chosen according to the cumulative energy, ϵ, as done in [15]. The cumulative energy is defined as $\epsilon(n) = (\sum_{i=1}^{n}\lambda_i)/(\sum_{i=1}^{N}\lambda_i)$, where N is the total number of points used for the numerical integration of Eq. 2 and λ_i sorted in descending order. A cumulative energy of 0.95 resulted in 9 eigenmodes to build the Karhunen-Loève expansion, which implies that the number of uncertainties associated to the manufacturing tolerances is nine. These uncertainties are introduced by means of the coefficients $Z_i(\omega)$ in Eq. 1, which are random variables normally distributed with mean 0 and variance 1, i.e., $\mathcal{N}(0,1)$. Therefore, this UQ study is comprised of 11 *aleatory* uncertainties and 2 *epistemic* uncertainties.

The validation method accounts also for the numerical uncertainties due to the discretization error. These were computed using a Richardson extrapolation algorithm by resorting on the implementation in the tool ReFRESCO [11]. Numerical and model input uncertainties are combined as $\sigma_{\text{sim}} = \sqrt{\sigma_{\text{num}}^2 + \sigma_{\text{input}}^2}$ [1].

3.1 Computational Framework for CFD Solver Validation

Figure 1 shows the simulation workflow of the SU2 DakOta Quantification of Uncertainty (SU2DOQU) framework. It is a python tool built to couple the open-source suite Dakota for uncertainty quantification with the CFD solver SU2.

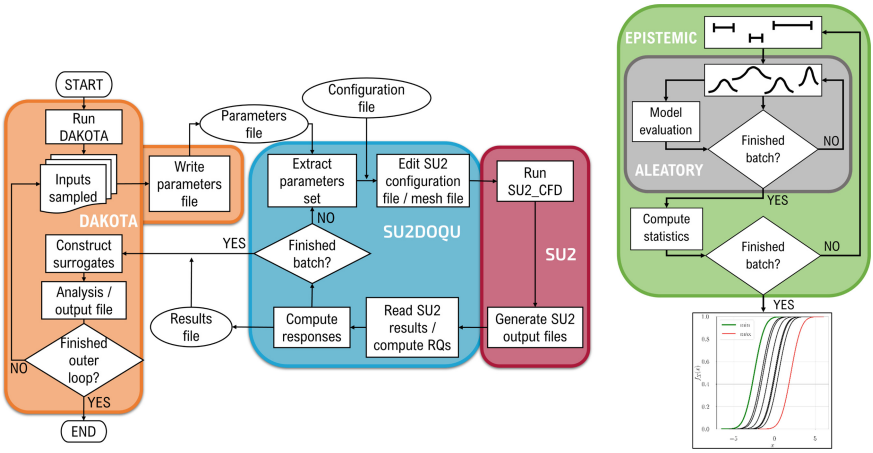

Fig. 1. SU2DOQU, Dakota and SU2 workflow (left) and flow diagram of the "Interval-valued" probability approach (right).

SU2DOQU implements two nested loops for treating both *epistemic* and *aleatory* uncertainties. The outer loop embeds an "Interval-valued" probability method for the *epistemic* uncertainties. No probability is assigned to these uncertainty sources, but a finite set of critical pressure and temperature pairs is selected from the defined intervals with a Latin hypercube sampling (LHS) method. For each pair of critical properties, the input *aleatory* uncertainties are propagated with a stochastic collocation method to calculate the cumulative probability of the chosen response quantities. The associated response functions are built by interpolation of the model predictions under different sets of sampled uncertain parameters. The interpolant used is value-based and thus the interpolation basis consist of the Lagrange interpolants. For a univariate case, where only one input uncertainty ξ is analyzed, the response functions are defined as

$$R(\xi) = \sum_{i=1}^{N} R(\xi_i) L_i(\xi) \qquad (6) \qquad \text{where,} \qquad L_i(\xi) = \prod_{j \neq i}^{N} \frac{(\xi - \xi_j)}{(\xi_i - \xi_j)}.$$

Here, N is the number of collocation points where the model response is evaluated, i.e., the number of sampled input uncertainties combinations. These combinations are generated using a method derived from tensor product quadrature, which uses tensor product of one-dimensional quadrature rules. However, for problems with a high number of input uncertainties this method results too computationally expensive. The Smolyak sparse matrices approach allows for the reduction in the number of collocation points by selecting only certain parameters combinations while keeping the accuracy of the tensor product quadrature approach. The level of the collocation points in the sparse grid matrix was set to be 3.

The ensemble of the cumulative density functions (CDFs) for the whole set of critical properties pairs is used to identify the maximum and minimum values of the response quantities. The final uncertainty bands of the simulations are built based on the obtained CDFs distribution. The lower bound is estimated by calculating the average of the CDF identifying the lowest values for the response quantity of interest and subtracting to this average twice the standard deviation of the corresponding CDF. An analogous procedure is adopted for the upper bound of the uncertainty bands.

4 Results

The static pressure at the nozzle wall (pressure taps locations are reported in [10]) and the Mach number along the centerline of the nozzle are the response quantities of interest. For each combination of critical point properties, a total of 2979 simulations were required to build the CDFs of the response functions with the stochastic collocation method. Figure 2 shows a family of CDFs corresponding to the sampled critical properties (ten pairs) for two exemplary quantities, namely the static pressure and the Mach number at the nozzle throat location. Similar trends were observed for other response quantities characteristic of other locations in the nozzle. As an example, the uncertainty band calculated for the static pressure at the nozzle throat, see Fig. 2a, is based on the two CDFs that are on the opposite sides of the chart, depicted in orange and purple, respectively. Notice that the CDFs are independent from each other and do not intersect. An extrapolation of their trend allows then to identify the two pairs of critical point properties that yield the maximum and minimum values for all the considered response quantities. In particular, the two combinations of critical point properties are [T_{cr}, P_{cr}] = [521.6 K, 18.9 bar] and [T_{cr}, P_{cr}] = [518.5 K, 19.27 bar]. The first pair is constituted by the minimum of critical pressure and maximum value of critical temperature, while the second pair is the other way around. The associated CDFs ensure that the computed uncertainty bands always include the effect of any combination of critical point properties in the considered interval. For this reason, the uncertainty bands associated to the simulation results have been computed considering only these two pairs.

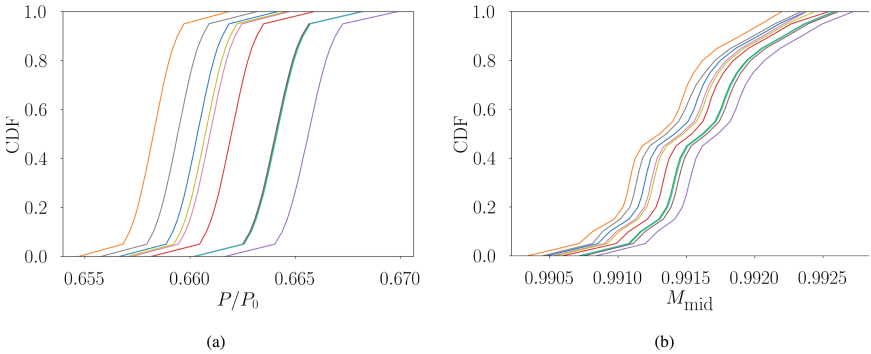

Fig. 2. CDFs corresponding to [518.72 K, 19.1 bar] —, [518.81 K, 19.33 bar] —, [519.82 K, 18.92 bar] — [520.53 K, 19.24 bar] — [521.18 K, 19.01 bar] — [521.41 K, 19.19 bar] — [519.29 K, 19.13 bar] — [519.63 K, 19.35 bar] — [518.81 K, 19.42 bar] — [520.14 K, 18.97 bar] —. **(a)** Family of CDFs for the pressure value at the nozzle wall at x = 0.0424 m from the inlet. **(b)** Family of CDFs for the centerline Mach number at x = 0.0424 m from the inlet.

Figure 3a shows the comparison between the calculated and measured static pressures along the nozzle with the corresponding uncertainty bands. The static pressure P is normalized with respect to the total pressure P_0 at the nozzle inlet, while the axial coordinate x is normalized with respect to the nozzle throat height H_{th}. The pressure distribution is well captured by the simulations. The average value of the measurements fall within the computed uncertainty bands except for a slight deviation at four locations within the kernel region of the nozzle (T09, T10, T13, T14). The maximum mismatch is observed at pressure tap T10 where the difference between the measured and simulated pressure is around 9 kPa. Possible causes of this deviation are a larger uncertainty in the throat size than that predicted by the manufacturing uncertainty model due to thermal effects, see [10], or 3D flow effects triggered by the boundary layer growth on the nozzle walls. Moreover, there is uncertainty related to the value of the nozzle back pressure, assumed fixed in the simulations. As shown also by the Mach distribution along the nozzle, in Fig. 3b, the flow is slightly over-expanded as proven by the two weak oblique shocks occurring in the final part of the channel. This effect is not quantified in the UQ study. Notice also that the uncertainty band width represents at most 1% of the average simulated pressure values, while that associated to the measurement is only 0.1%. This is the reason why the uncertainty bands of the pressure measurements are not visible in the Fig. 3a. The maximum uncertainty associated with the calculated pressure, ± 20 kPa, is found close to the throat, due to high sensitivity of throat location to manufacturing uncertainties.

Regarding the Mach distribution, the largest discrepancies are found in the straight part of the nozzle. Notably, the Mach number reduction due to the oblique shocks appears to be stronger in the experimental results. The reason thereof can be attributed again to the uncertainty associated to the nozzle back pressure. A maximum deviation of around 0.045 between the simulated and experimental Mach number is observed in correspondence of the first shock. Similarly to the uncertainty in the pressure profile, the

largest uncertainty band in the simulated Mach number, that is around 0.015, is found close to the throat due to the uncertainty in the throat location caused by manufacturing inaccuracies.

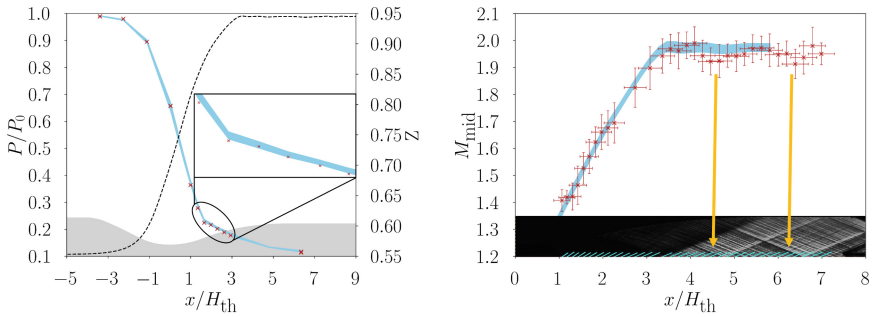

Fig. 3. Comparison between simulation ( ) and experimental results (x). The simulation uncertainty was computed and the limits of the uncertainty band correspond to $[X_{\max} + 2\sigma_{\text{sim}}, X_{\min} - 2\sigma_{\text{sim}}]$, where $X_{\max}$ and $X_{\min}$ are the maximum and minimum average values of each response quantity corresponding to the different combinations of critical point properties. **(a)** Static pressure along the nozzle wall. Upper and lower wall pressure taps data is compared to the nozzle wall pressure of the simulation. The centerline compressibility factor (- -) is shown together with a zoomed-in section of the kernel region. **(b)** Centerline Mach number in the diverging part of the nozzle. A comparison with the schlieren image taken during the experiment is also shown.

5 Conclusions

In this paper, experimental pressure and Mach number data from a non-ideal isentropic supersonic expansion have been compared against the numerical results from the open-source fluid dynamic solver SU2 using an in-house uncertainty quantification framework for aleatory and epistemic uncertainties called SU2DOQU. A good match between the experimental and numerical Mach number and pressure trends was found. The maximum deviation in the pressure distribution is about 1% and occurs in the kernel region. The reason can be attributed to small differences in the area distribution and expansion ratio of the nozzle between experiment and simulations. This mismatch could be reduced by measuring the nozzle area distribution during the experiment and better characterizing the outlet static pressure of the nozzle. Similar considerations hold for the Mach number distribution, though the maximum deviation is found to occur in the straight final part of the nozzle, where two weak oblique shock waves appear. Future work will target a more comprehensive validation campaign involving experiments in other non-ideal thermodynamic conditions and the possible use of more accurate CFD models and fluid equations of state.

References

1. American Society of Mechanical Engineers (ASME) 2009 Standard for Verification and Validation in Computational Fluid Dynamics and Heat Transfer. Technical report V&V20-2009. ASME (2009)
2. Betz, W., Papaioannou, I., Strauss, D.: Numerical methods for the discretization of random fields by means of the Karhunen-Loève expansion. Comput. Methods Appl. Mech. Eng. **271**, 109–129 (2014)
3. Bills, L.: Validation of the SU2 flow solver for classical NICFD. Master's thesis, Delft University of Technology (2020)
4. Celik, I.B., Ghia, U., Roache, P.J., Freitas, C.J., Coleman, H., Raad, P.E.: Procedure for estimation and reporting of uncertainty due to discretization in CFD applications. J. Fluids Eng. **130**(7) (2008)
5. Dickinson, E., McLure, I.A.: Thermodynamics of n-alkane + dimethylsiloxane mixtures. part 3.-excess volumes. J. Chem. Soc., Faraday Trans. 1 **70**, 2328–2337 (1974)
6. Dow, E., Wang, Q.: Optimal design and tolerancing of compressor blades subject to manufacturing variability. In: 16th AIAA Non-Deterministic Approaches Conference (2014)
7. Economon, T.D., Palacios, F., Copeland, S.R., Lukaczyk, T.W., Alonso, J.J.: SU2: an open-source suite for multiphysics simulation and design. AIAA J. **54**(3), 828–846 (2015)
8. Gori, G., Zocca, M., Cammi, G., Spinelli, A., Congedo, P.M., Guardone, A.: Accuracy assessment of the non-ideal computational fluid dynamics model for siloxane MDM from the open-source SU2 suite. Eur. J. Mech. - B/Fluids **79**, 109–120 (2020)
9. Head, A.J.: Novel experiments for the investigation of non-ideal compressible fluid dynamics: The orchid and first results of optical measurements. PhD thesis, Delft University of Technology (2021)
10. Head, A.J., et al.: Mach number estimation and pressure profile measurements of expanding dense organic vapors. In: Pini, M., De Servi, C., Spinelli, A., di Mare, F., Guardone, A. (eds) Proceedings of the 4th International Seminar on Non-Ideal Compressible Fluid Dynamics for Propulsion and Power. NICFD 2022. ERCOFTAC Series, ERCO, vol. 29, p. IX, 240. Springer, Cham (2023)
11. Marin (2019). https://www.refresco.org/verificationvalidation/utilitiesvvtools/
12. McLure, I.A., Dickinson, E.: Vapour pressure of hexamethyldisiloxane near its critical point: corresponding-states principle for dimethylsiloxanes. J. Chem. Thermodyn. **8**(1), 93–95 (1976)
13. Nyström, E.J.: Über die praktische auflösung von integralgleichungen mit anwendungen auf randwertaufgaben. Acta Math. **54**, 185–204 (1930)
14. Pini, M., et al.: SU2: the open-source software for non-ideal compressible flows. J. Phys: Conf. Ser. **821**, 012013 (2017)
15. Razaaly, N., Persico, G., Congedo, P.M.: Impact of geometric, operational, and model uncertainties on the non-ideal flow through a supersonic orc turbine cascade. Energy **169**, 213–227 (2019)
16. Vitale, S., et al.: Extension of the SU2 open source CFD code to the simulation of turbulent flows of fluids modelled with complex thermophysical laws. In: Proceedings of the 22nd AIAA Computational Fluid Dynamics Conference (2015)
17. Woodward, S.D., Dury, M.R., Brown, S.B., McCarthy, M.B.: Understanding articulating arm laser line scanners for precision engineering: operator usage effects. In: Proceedings of the ASPE 2015 Annual Meeting (2015)